DEVELOPMENT OF A STANDARD RETICLE TARGET FOR CALIBRATION OF MALDI IMAGING MASS SPECTROMETRY INSTRUMENTS

By

Patrick Dale Rawhouser

Thesis

Submitted to the Faculty of the

Graduate School of Vanderbilt University

in partial fulfillment of the requirements

for the degree of

MASTER OF SCIENCE

in

Chemistry

December, 2012

Nashville, Tennessee

Approved:

Professor Richard Caprioli

Professor Carmelo Rizzo

ACKNOWLEDGEMENTS

This work was supported by NIH/NIGMS grant 8P41 GM103391-02. I would like to thank Dr. Junhai Yang for his help with the organic molecules, Dr. Andre Zavalin and Erik Todd for help working the modified AB 4700 instrument, and the MSRC for help and support throughout this work. I would also like to thank Dr. Paul Laibinis for his guidance with the surface chemistry aspect of this project, without whose assistance, this work would not have been possible. I would also like to thank my friends, Chad "chumbles" Chumbley, David Rizzo, Erik Todd, Jessica Moore-Hooten, David "Asian Dave" Crisostomo, Jeremy "Clean" Beam, Bobby Boer, and Alex Raubach for keeping my spirits light and my days enjoyable.

Nobody has been more important to me in the pursuit of this project than the members of my family. I would like to thank my parents, whose love and guidance are with me in whatever I pursue. They are the ultimate role models. Most importantly, I wish to thank my loving and supportive girlfriend, Meghan.

TABLE OF CONTENTS

ACKNOLEDGEMENTS……ii

LIST OF FIGURES……iv

Chapter

I. INTRODUCTION……1

II. CREATION OF A STANDARD TARGETING RETICLE……4

Initial work on the creation of the targeting reticle……4
Materials……4
Methods used to create the standard slide……4
Verifying the measurements of the slide……6
Verifying the slide using mass spectroscopy……7
Results……7
Depositing an organic solution to create the slide……7
Patterning traditional MALDI matrices……9
Simple detachment patterning of an organic molecule……11
Verification of the slide……13
Initial experiments in MALDI instrumental calibration……13
Determination of laser beam size……15
Accuracy test……16
Comparison of multiple measurement platforms……17
Summary……19

BIBLIOGRAPHY ……21

LIST OF FIGURES

Figure Page

1. Fabrication of IMS reticle……6
2. Crystal violet pattern formed using different methods……8
3. Sublimed DHB target……10
4. Patterned Rubrene made from simple detachment patterning……12
5. Image comparison between optical, fluorescence, and ion images ……14
6. Determination of effective laser spot size from UltrafleXtreme……15
7. Accuracy test performed on the UltrafleXtreme……16
8. Intensity comparison between UltrafleXtreme, Fluorescence, and 4700……18
9. Resolution test for the 4700 at 1 µm……19

CHAPTER I

INTRODUCTION

The need exists to accurately compare the performance characteristics of Matrix Assisted Laser Desorption/Ionization (MALDI) Time of Flight (TOF) instruments in terms of performance parameters, such as the laser beam and raster step size, that are routinely set in the acquisition software prior to imaging. These are necessary parameters to validate, independent of the supplied manufacturer software, and are necessary for standardization of data reported from different laboratories. Since the beginning of Imaging Mass Spectrometry (IMS)[1], accurate stage movement and laser alignment have been paramount concerns to validate the generated images. With the rise of commercial instrumentation, calibration and validation of important physical parameters of the system are often left to the control of instrument software. Imaging instruments are now routinely used for the detection of a wide range of compounds, including peptides[2], proteins[3], and lipids[4] on instrument types that may include TOF[5], Fourier transform ion cyclotron resonance (FT-ICR)[6],Linear trap quadrupole (LTQ)[7], ion mobility[8], as well as many others.

The wide variety of different instrument models available render it improbable that each instrument is calibrated to the same specifications. Even between instruments of the same model that employ the same laser type and settings, the instrumental parameters can differ due to variations in the laser optics and other instrument specific parameters. Different operating conditions can and do lead to slight changes to resolution and laser fluence thus leading to artifacts showing up in images which can be misinterpreted by the user. A standard calibration reticle is needed to standardize the data from the operating conditions seen in various

laboratories such that comparisons between labs can be made without regard to the differences in operating conditions.

In order to measure the effective laser size and resolution of a MALDI imaging instrument quickly and easily, and have the measured data be comparable between labs, test targets are needed that have pre-defined spatial information that can be accurately measured and independently verified. While targets for this purpose exist for Secondary Ion Mass Spectrometry (SIMS) imaging[9], the nanometer size of the features renders them too small for the calibration of most MALDI instruments.

If one considers the ideal test target, an important considerations to take into account are that the surface compound to be used is easily ablated yielding a high ion intensity and that features of the pattern be completely resolved from one another. There are two ways to ensure that the features of the target are completely resolved from each other: using chemical or physical barriers while depositing material and removal of excess material to create a pattern. Photolithography was considered for the use of physically separating the material, however, it was deemed too expensive to make on a large scale. By forming a chemical pattern using hexadecanethiol stamped on a gold surface, multiple types of organic compounds could be used to create the features in the hydrophilic regions of the gold. By using a PDMS mold, some hydrophobic organic molecules, including rubrene, could be easily patterned[10] to sub-micron sizes[11]. These can be easily detected by mass spectrometry, and easily visualized using fluorescence imaging[12,13]. For the purpose of creating a standard target, I explored a number of methods: the deposition of crystal violet and sinapinic acid (SA) on a pre-patterned thiol coated gold surface and removing 1,5 diaminonapthalene (DAN) matrix and rubrene.

This report describes the development of a standard slide, validation of the resolved pattern using fluorescence imaging, as well as a procedure for determining the effective laser spot size and IMS resolution from the pattern. Moreover, the patterned slide is shown to be effective on a commercial MALDI TOF instrument, Bruker UltrafleXtreme, at raster step sizes down to 15 µm and on a modified AB 4700 MALDI TOF instrument at raster step sizes down to 1 µm.

CHAPTER II

CREATION OF A STANDARD TARGETING RETICLE

Initial work on the creation of the targeting reticle

Materials

Crystal violet, hexadecane thiol, and DAN were purchased from Sigma-Aldrich (St. Louis, MO) and used as delivered. Rubrene was purchased from Alfa Aesar (Ward Hill, MA) and used as delivered. For this experiment, the poly(dimethylsiloxane) (PDMS) pattern consisted of squares at a constant 100 μm pitch that decreased in their length and width by 1 μm from 100 μm to 2 μm with each row and was made using standard procedures[14]. The gold slides were purchased from Deposition Research Laboratory Inc (St. Charles, MO) and were washed with isopropanol prior to use. The ITO slides were purchased from Delta Technologies and were cleaned by sonication in 1% Triton X-100 solution, acetone, and isopropanol for 5 min each prior to use.

Methods used to create the standard slide

Crystal violet was dissolved in ethanol at 30 mg/ml and spread across a pre-patterned PDMS mold using a cotton swab to produce a thin layer. The dissolved crystal violet was allowed to dry for 30 seconds and was then pressed lightly onto a cleaned ITO coated glass slide. The mold was held in place manually with light pressure for 1 minute and then removed. The slide was inspected using an optical profilometer from Zeta (San Jose, CA) for cleanliness and resolution of the pattern. Additionally, crystal violet was spun onto a cleaned ITO slide using a ramping program of 10 seconds to a maximum of 4000 rpm. The slide was then baked at 80°C for 2 minutes to remove the ethanol. Next, the slide was either placed into the oven for 1 hour

at 90°C with a PDMS mold on top of it to remove the excess crystal violet or the mold was pressed onto the slide to remove crystal violet immediately.

A 2 mM ethanol solution of hexadecane thiol was prepared and spread over the PDMS mold in the same manner as the crystal violet solution. The mold was placed onto a cleaned gold coated slide and pressed into complete contact. After 30 seconds, the mold was removed from the slide and excess thiol was washed away using ethanol and DI water. Initially, on these thiol coated slides, crystal violet was deposited using the T-BAG[15] method of allowing the solution to evaporate over the slide held vertically. In addition, it was found a thin layer of crystal violet could be deposited in a pattern by placing a droplet of less than 5 µl of crystal violet solution on the side of the slide and tilting the slide to allow the liquid to run over the hydrophilic features.

Sinapinic acid was grown on the hydrophilic regions of a thiol coated slide by immersing it in a solution of Carnoy's fluid. In this case, the Sinapinic acid attaches to the unmodified gold and allows the matrix crystals to grow from this starting material. These slides were also inspected using an optical profilometer from Zeta instruments for the resolution of the pattern.

A thin film of rubrene was sublimed onto a cleaned ITO glass slide using a Chemglass sublimation apparatus[16] in a sand bath at 230°C for 15 min at 80 mTorr. After the sublimation was complete, the slide was warmed to room temperature and dried under a stream of air and placed in a vacuum desiccator for 30 minutes. Next, a pre-patterned PDMS mold was placed on top of the rubrene, gently pressed into conformal contact, and the slide with the mold was heated to 90 °C for 45 min (Figure 1A-D). After allowing the slide to cool, the PDMS mold was removed from the slide by hand causing the regions of rubrene that were in contact with the PDMS to detach from the slide[10] producing the calibration target.

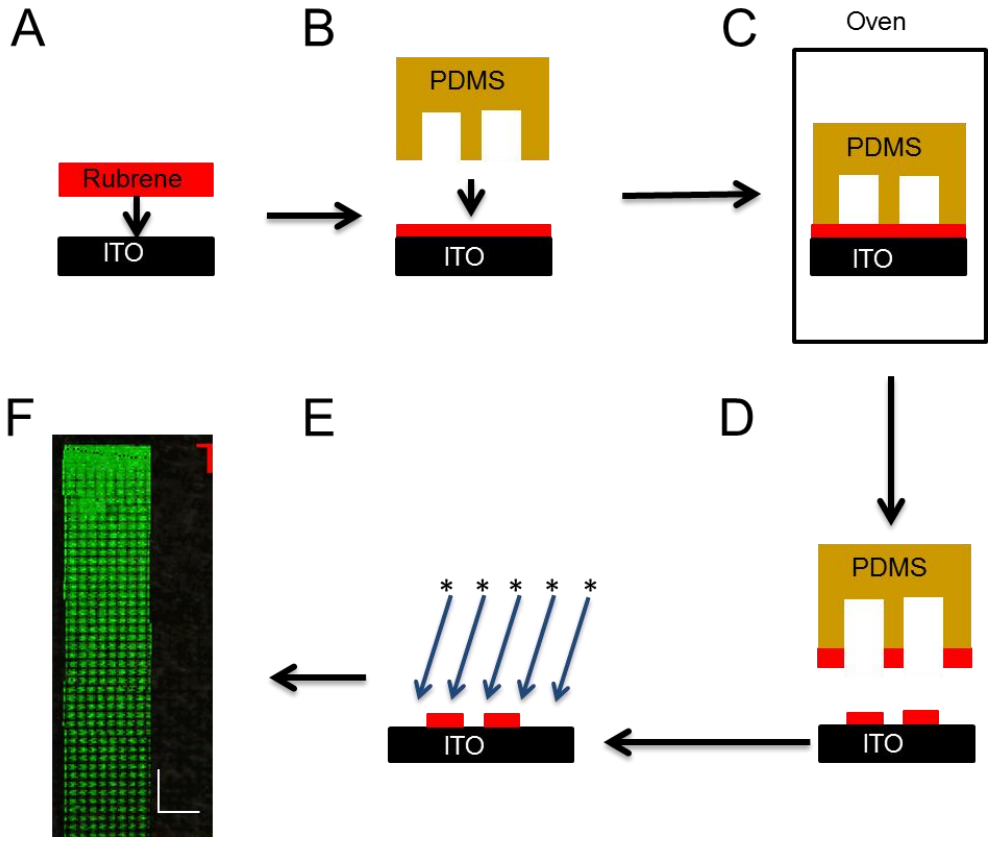

Figure 1: Fabrication of IMS reticle: (A) rubrene is sublimed onto the cleaned ITO slide and (B) the PDMS stamp is placed onto the slide. (C) The slide is then placed into the oven at 90°C and then (D) the PDMS stamp is removed, which also removes rubrene that was in contact with the stamp. (E) The pattern is then imaged and (F) analyzed using flexImaging, scale bar is 500 µm

A thin layer of DAN was sublimed onto a cleaned ITO glide using the Chemglass sublimation apparatus at 120°C for 6 minutes at 80 mTorr. The removal of DAN followed the same procedure as the removal of rubrene stated above.

Verifying the measurements of the slide

Before preforming imaging mass spectrometry, the pattern was measured using a Zeta-20 optical profilometer and a Nikon Eclipse 90i microscope using a DAPI fluorescence filter. This

enabled the accurate determination of the thickness of the sample as well as the distances across and between each feature. These measurements are crucial to determine the reproducibility of the sublimation and correlation between the pattern and the ion image.

Verifying the slide using mass spectroscopy

MALDI-IMS was performed on an UltrafleXtreme MALDI-TOF/TOF (Bruker Daltonics, Billerica, MA) in reflection mode under optimized conditions and at its minimum beam diameter setting. MS data resulted from summing the signals from 300 laser shots per x-y coordinate (Figure 1E). The images were automatically acquired at various raster step sizes at 15%, 25%, and 50% laser energy and were reconstructed using FlexImaging 3.0 software (Bruker Daltonics).

Ultra-high resolution imaging was done on an AB 4700 instrument modified to have transmission geometry and produce laser spot sizes below 1 µm. A custom designed vacuum compatible inverted optical/laser microscope with its z-axis parallel to the z-axis of the mass-spectrometer was used to focus a laser beam inside an analyte layer through a transparent substrate, thus reducing the beam to micron sizes[17]. Images were acquired with a 1 µm raster step size. The MS data were summed from 25 laser shots and the images were reconstructed using BioMAP 3 (Novartis Institutes, Basel, Switzerland).

Results

Depositing an organic solution to create the slide

Initially, I wanted to start with the method that could prove to be the simplest and cheapest if it proved successful: stamping an organic solution onto an ITO slide. For the first experiment, a solution of 30 mg/ml was prepared and spread over the PDMS mold and the mold was pressed onto the ITO slide. It was noted that the solution was too thick and spread across

the surface of the slide leaving no discernible pattern. The next test attempted focused on reducing the amount of solution applied to the mold. Unfortunately, the pattern still did not appear on the slide. And so, various concentrations of crystal violet were made in order to determine which provided the appropriate viscosity for stamping. Even with the changes in viscosity, the crystal violet did not form a viable pattern with this method. Spin coating the crystal violet onto the ITO slide was next attempted in order to generate a homogenous coating over the slide and then using the PDMS mold to remove the excess material to create the desired pattern. When the slide was placed in the oven, no patterning was seen with the crystal violet as has been reported with other organic compounds[10]. Using the PMDS mold without added heat yielded a pattern, but it was not consistent below 60 µm and did not show good resolution of the features (Figure 2A). This removal technique showed promise if I could determine the correct material to use.

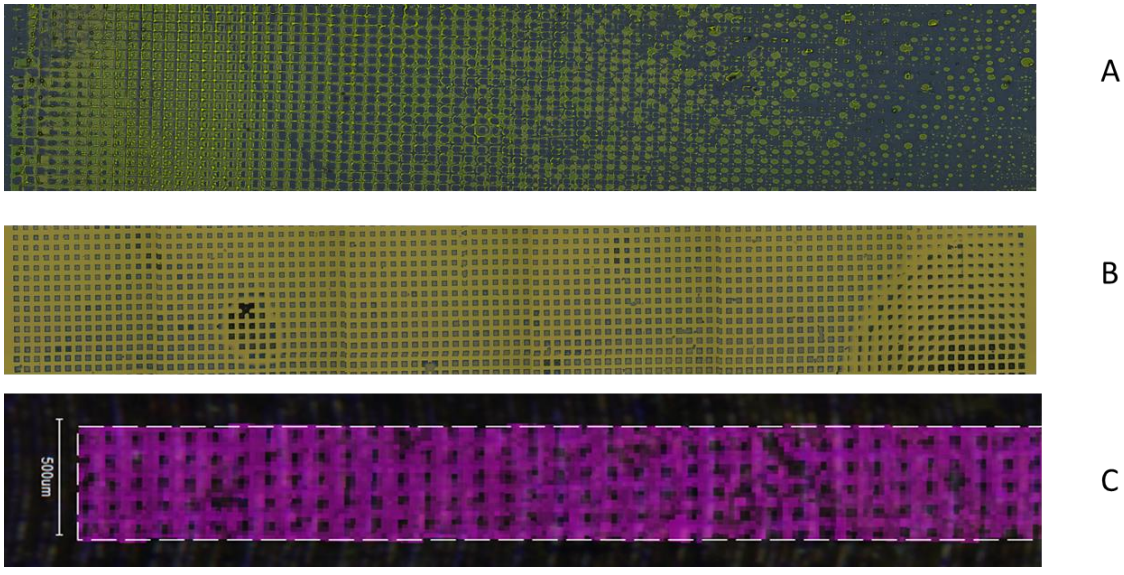

Figure 2: Pattern of crystal violet formed after (A) pressing a PDMS mold onto a spin-coated surface, (B) using hydrophobic thiol to create a pattern for the crystal violet to be deposited, and (C) the ion image (m/z 372.32) of the middle of the pattern in (A) from the Bruker UltrafleXtreme

On the other hand, by modifying the surface hydrophobicity of a gold slide, crystal violet will only deposit in the hydrophilic regions, which would be the pattern. To begin with, the gold surface was modified with a solution of 2 mM hexadecane thiol on a pre-patterned PMDS mold with 100 µm indentions at 150 µm pitch. The success of the modification was tested by immersing the slide in ethanol and since the majority of the slide is hydrophobic, with only the patterned areas being hydrophobic, most of the ethanol will run off the slide except for the patterned area. After the modification, the slide was immersed in a solution of crystal violet and ethanol. However, there was too much solvent for the pattern to be resolved by the time the ethanol evaporated. Even holding the slide vertically to allow the solution to run off the slide didn't allow the pattern to be completely resolved when the ethanol evaporated.

The next experiment was to allow the crystal violet solution to evaporate down the slide slowly over the course of a night using a modified T-BAG method[15]. Unfortunately, this method did not resolve the problem of having too much solution left over on the slide and, therefore, I decided to deposit crystal violet on the pattern using a small amount of solution. To do this, I pipetted 5 µl of the crystal violet solution onto the edge of the thiol patterned gold slide and tilted the slide slightly to allow the droplet to roll over the patterned area. This method allowed the solution to deposit material in the hydrophilic features without overflowing the slide with solution. However, it did not yield a consistent amount of material left in the pattern nor were I able to generate a large pattern using this method (Figure 2B).

Patterning traditional MALDI matrices

Because I was not able to make a consistent and reproducible pattern using the deposition of crystal violet onto a modified gold target, I began working on a way to pattern traditional MALDI matrices. The initial experiment in patterning matrices was to determine if

commonly used matrices are suitable for use in the pattern. To do this, I sublimed a layer of DHB onto a cleaned ITO slide and used a laser capture microdissection (LCM) instrument to generate a small pattern in the DHB, as seen in Figure 3A. The pattern was then imaged under standard imaging conditions at a raster step size of 10 µm with the resulting image (*m/z* 157.97) seen in Figure 3B. The pattern was reproduced in the ion image very accurately. Because of the length of time required for patterning a relatively small area using the LCM, a different method for making the features needed to be used.

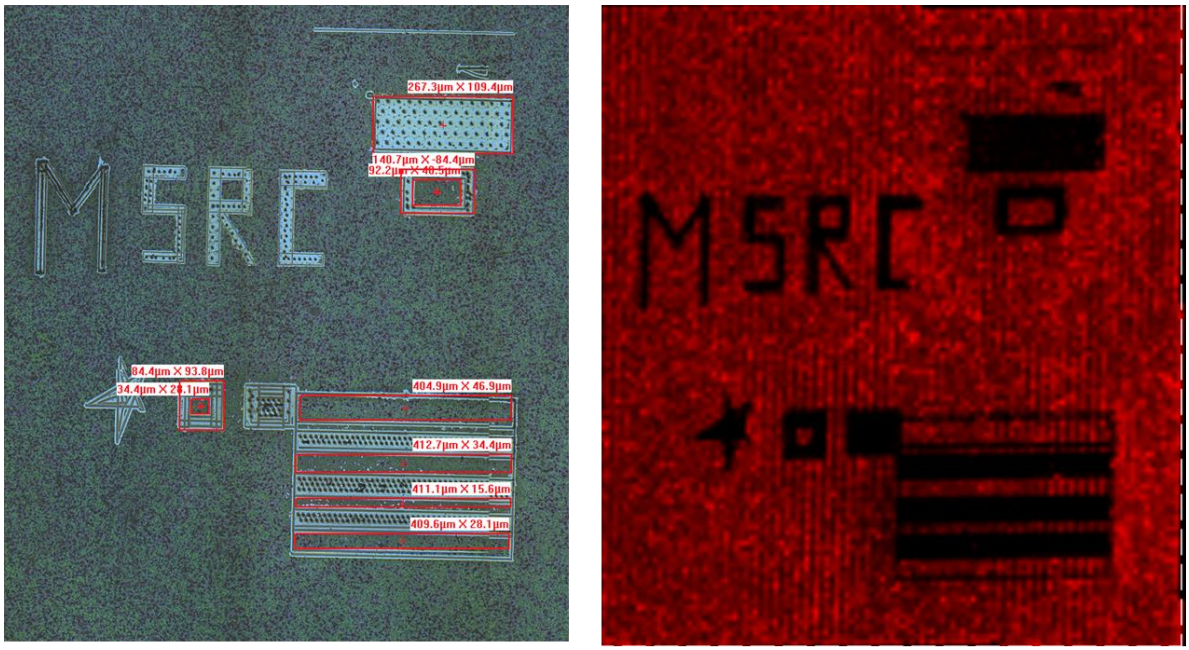

Figure 3: (A) Target created using a sublimed layer of DHB with the LCM and (B) the resulting ion image from the DHB generated on the Bruker UltrafleXtreme

By modifying the gold using the same thiol method as above, I was able to grow the matrix in the same regions that I deposited crystal violet previously. Unfortunately, traditional

MALDI matrix compounds (Sinapinic acid, 2,5-dihydroxybenzoic acid, and α-cyano-4-hydroxycinnamic acid) are not favored because they are not easily patterned at the feature sizes required for this calibration target, nor are they able to be independently verified regarding the size and shape of the pattern, other than optically. Optical microscopy may not be sensitive enough to detect material that would be readily detected in IMS experiments should any material remain between the features. In addition, many matrices form crystals that give rise to inhomogeneous surfaces[18].

Simple detachment patterning of an organic molecule

While I was looking for a method to pattern organic materials quickly and with high reproducibility, I discovered simple detachment patterning[10] which allows the patterning of organics for use in the semi-conductor industry. Because the method of detachment requires a hydrophobic molecule to bind to the hydrophobic PDMS mold, most of the matrices that are traditionally used for MALDI experiments would not be appropriate. However, DAN was found to be both hydrophobic and a suitable matrix[19]. Because the layer of matrix needed to be thin enough to detach properly with the PDMS mold, multiple combinations of time and temperature for sublimation were attempted before finding the optimal of 6 minutes at 120°C followed by 60 minutes in a 90°C oven for detachment. Unfortunately, the DAN had a cohesion strength that was greater than the adhesion strength between it and the PDMS mold. This resulted in most of the matrix being removed while only small amounts remained on the slide. Finally though, the DAN was not completely resolved and was not easily detected in the UltrafleXtreme TOF/TOF instrument, two criteria that are critical to the success of the target.

5,6,11,12-tetraphenylnaphthacene (rubrene) was determined to be the most likely compound to be photoactive in the UV region of the lasers used to induce

desorption/ionization. To test this, rubrene was dissolved in acetone and hand-spotting onto an ITO slide. The rubrene was easily detected in the mass spectrometers. Due to the fact that rubrene is practically insoluble in most traditional solvents, sublimation was chosen to coat the targets with a layer of rubrene. Because of the high melting point of rubrene, the sand bath of the sublimation apparatus had to be heated to 230°C and dry ice with acetone was substituted for ice in the cold finger in order to cool the substrate. Various times were tested for the deposition of a thin layer of rubrene to facilitate detachment. The optimal time for sublimation was 15 minutes followed by 45 minutes in a 90°C oven. After removal of the PDMS mold, the rubrene pattern reproduced the PDMS pattern accurately with features visible below 10 µm (Figure 4).

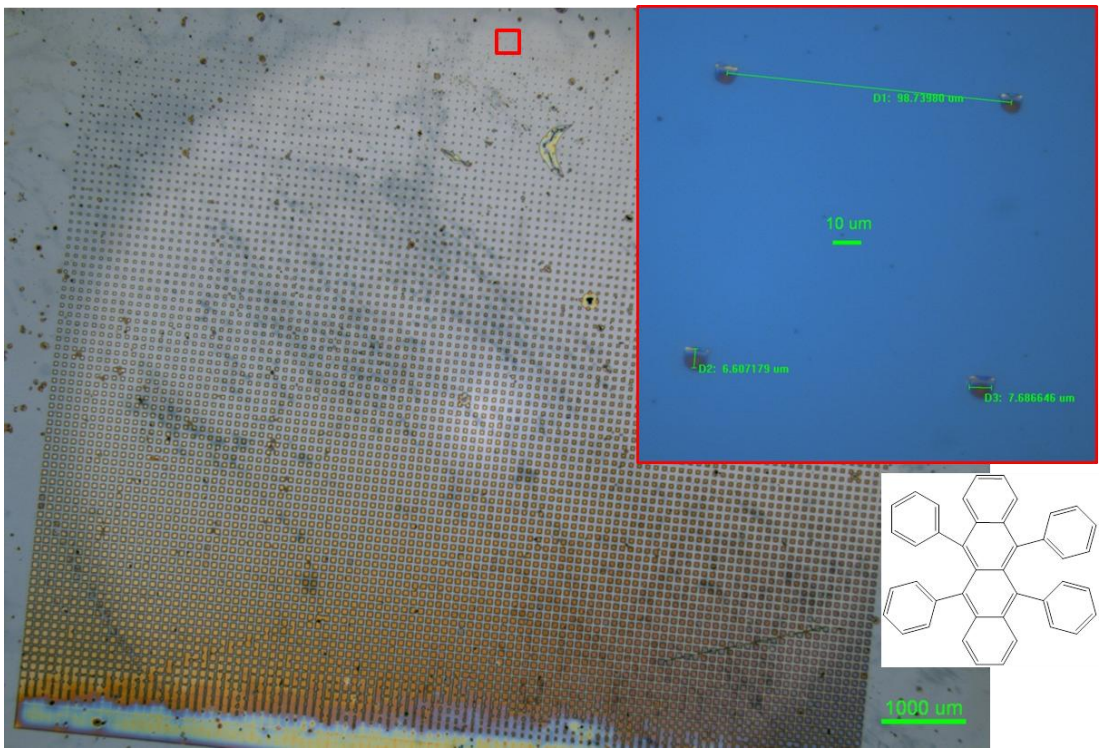

Figure 4: Patterned rubrene (structure in the lower right) made by simple detachment patterning with good reproducibility and the ability to generate features below 10 µm (insert zoomed 150X).

Verification of the slide

After experimentation, I adopted the detachment patterning of rubrene approach that has been shown to generate reliable sub-micron-sized features of rubrene[11] for fabricating the IMS standard. The reproducibility of the thickness and amount of the sublimed rubrene is important to maintain consistency in the data generated from imaging experiments. Over the time periods tested in this experiment, 15 min proved to be the optimal time to sublime rubrene at 230°C at 80 mTorr to create a regular pattern of rubrene after detachment patterning with an average of 0.073 $\pm$ 0.025 mg/cm^2 of rubrene deposited onto the ITO slide. By using an optical profilometer, the corresponding thickness of the rubrene was found to be 380 $\pm$ 130 nm (a representative optical image is shown in Figure 5A). In addition, through the use of fluorescence, I were able to verify that rubrene between the features in the pattern was removed during the detachment process (Figure 5B). As shown in Figure 2C, the ion images correlated well to the optical and fluorescence images.

Initial experiments in MALDI instrumental calibration

Figure 6 shows an image of the rubrene pattern taken from the UltrafleXtreme MALDI TOF instrument at minimum beam setting. The pattern of rubrene was divided into four regions for imaging at four different raster step sizes: 15, 25, 50, and 75 μm. The pattern was analyzed by finding at what raster step size oversampling began. Since each region should have the same amount of rubrene within it due to imaging identical sections of the pattern, the intensity of rubrene (*m/z* 532.2) from the average spectrum from each of these regions should be consistent in each region; however, oversampling would cause a decrease in the intensity of rubrene in average spectrum of a particular region. Plotting the overall average intensity of the rubrene peak from each region against the raster step size, the region where oversampling began can be

determined. It was found that oversampling began with the 25 µm region, and therefore the effective laser beam size was somewhere between 25 and 50 µm.

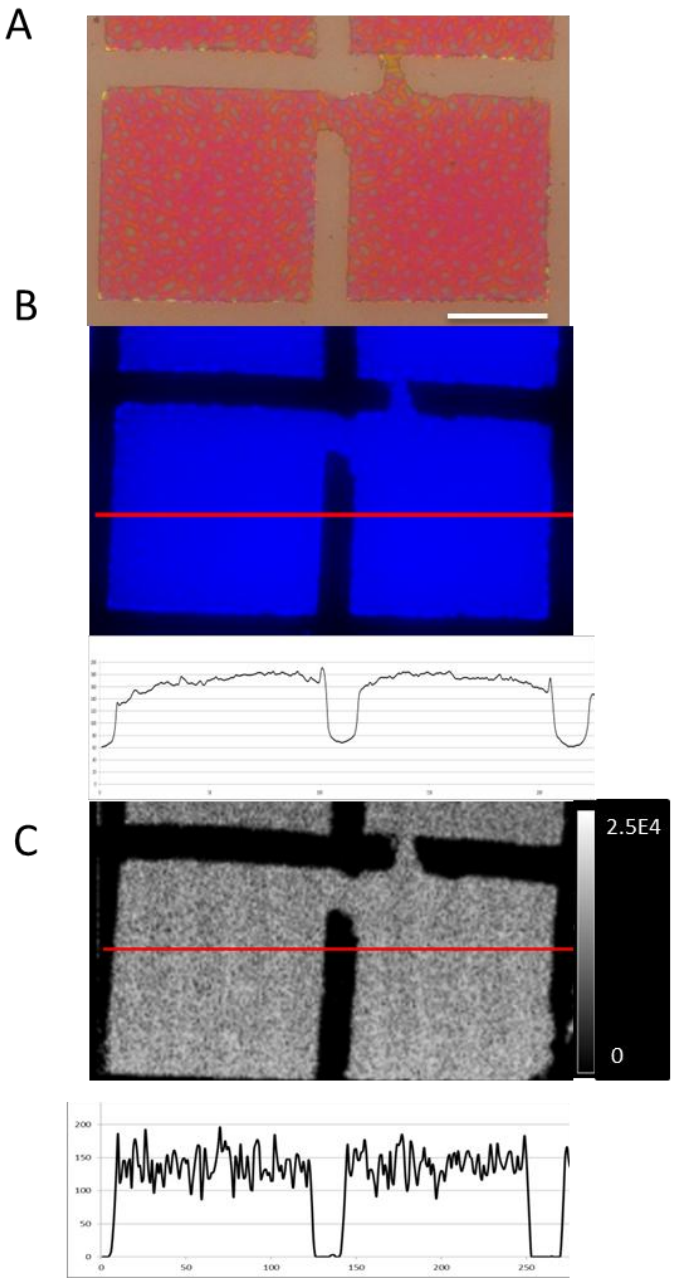

Figure 5: The (A) optical, (B) fluorescence, and (C) ion images from the 4700 with intensity profiles for the fluorescence and ion images of the reticle. The scale bar seen in A is 50 µm. Note: the defect seen in the images was used as a point of reference when dealing with both images and corresponding profiles

Determination of laser beam size

A more precise beam size can be determined by finding the part of the pattern where the features of rubrene are completely resolved in the ion image. This correlates to the section of the pattern where the laser beam size is less than the gap between the features. In this experiment, the area imaged consisted of rubrene features varying in length from 85 µm (top) to 55 µm (bottom), corresponding to 15 µm – 45 µm spacing between the rubrene features. The features became completely resolved in this image at the 65 µm feature, which means that the laser spot size is equal to or less than the distance between the features, or 35 µm.

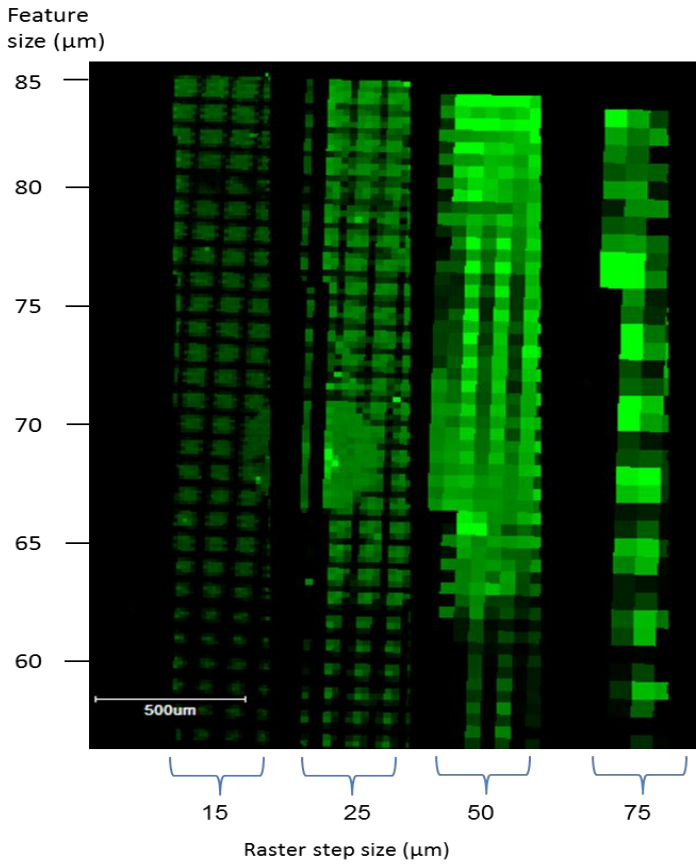

Figure 6: Ion image from UltrafleXtreme at m/z 532.2 using multiple raster step sizes to determine the effective laser spot size of the instrument based on oversampling and the resolution of the pattern. Normalized to TIC

In order to test the target more thoroughly, the laser power was doubled in order to increase the laser size on the target. After repeating this experiment as various laser intensities, a calibration line can be generated correlating the effective spot size with laser power. Although the instrument ages and the effective settings change, the software settings remain constant. By generating a curve such as this over time, the effective spot size can be accurately measured as the effective settings change. By carrying out this test at regular intervals, the performance of each instrument can be easily assessed.

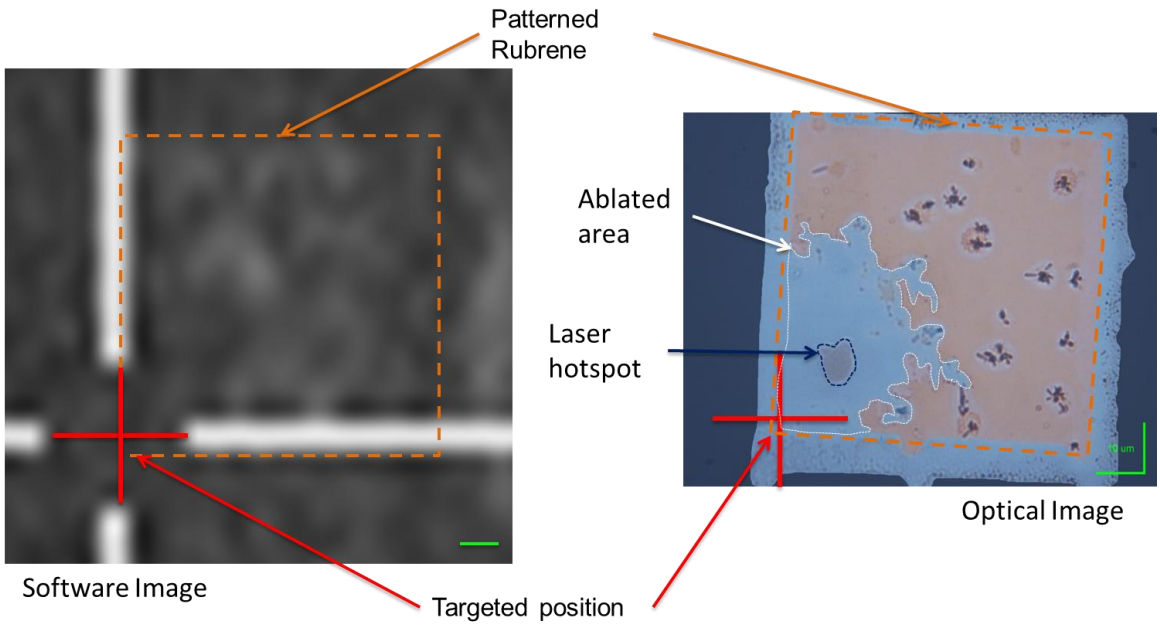

Figure 7: Accuracy test using the patterned rubrene images from both the software's targeting system and the corresponding optical image, which allows the user to measure the amount the laser was off from the targeted position.

Accuracy tests

The accuracy of the laser positioning software was also tested using this pattern of rubrene. Normal calibration of the laser positioning software is performed by using a coating of

matrix, firing the laser into that coating, and aligning the laser with the created hole. However, due to the distance between the crosshairs, the deviation in the expected position and the actual position may allow for missing the region to be imaged, especially at high resolution. Measuring the difference between the expected position and the actual position will allow the deviation in the targeting software for individual instruments to be calibrated and reported. By placing the targeting crosshairs on the lower left corner of one of the boxes of rubrene, the expected position of the laser is known while inspecting the pattern using optical microscopy. The laser hotspot was assumed to be the center of the laser shot, from which the deviation from the expected placement can be determined. A side-by-side comparison is shown in Figure 7. For this UltrafleXtreme II instrument, the laser position software was off of the actual placement of the laser by 9.7 µm in the x direction and 12.0 µm in the y direction.

Comparison of multiple measurement platforms

Figure 8 shows the intensity profile across a feature in the rubrene pattern of the standard slide using data from three different instruments: the UltrafleXtreme imaged at 15 µm, the modified 4700 imaged at 1 µm, and the fluorescence microscope. The fluorescence and the 4700 profiles were very similar due to the similar resolution, although the intensity of the ions in the 4700 was much more variable than what was seen in the fluorescence. The broader profile was generated by the UltrafleXtreme because of the large raster step size. All three profiles generated a consistent length of the feature of the intensity profile as measured at full width half maximum (FWHM) of approximately 70 µm.

In order to demonstrate the utility of the rubrene standard pattern, a small area was imaged on a modified AB4700 instrument at 1 µm raster step size and the resulting image is shown in Figure 5C with the corresponding ion intensity profile of rubrene. The defects seen in

the pattern represented an opportunity to test the system by measuring small defects using the profilometer and fluorescence prior to MS.

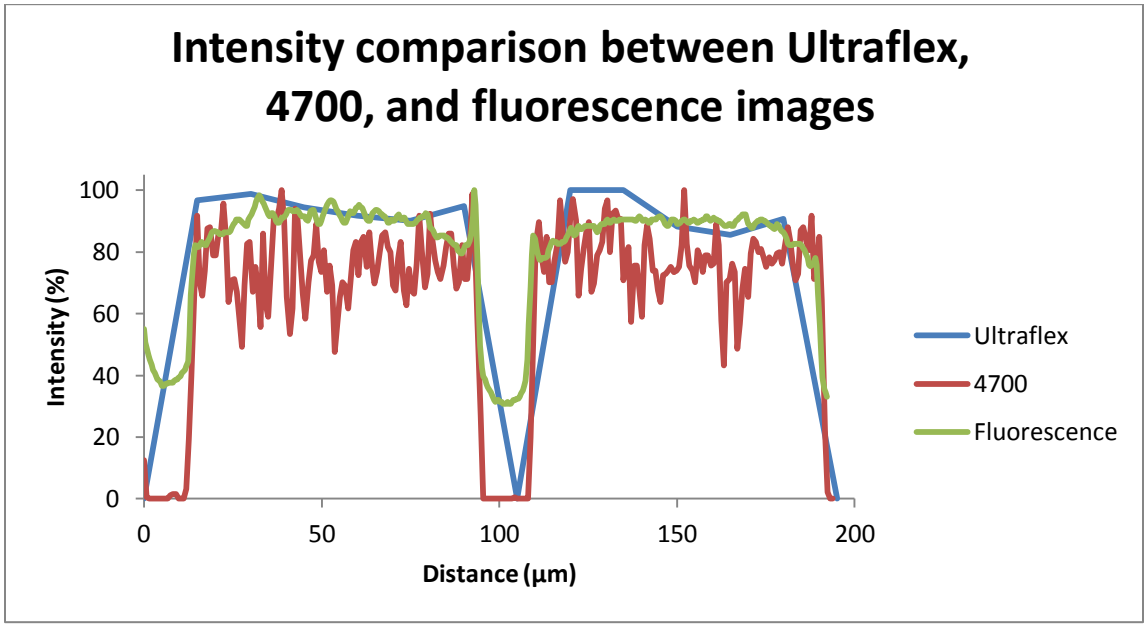

Figure 8: Overlaid graph showing the profile of a rubrene feature as measured by the UltrafleXtreme at 15% laser energy (blue), the modified 4700 (red), and fluorescence imaging (green)

The comparison of the optical and ion images showed the defects reproduced correctly in the 1 µm image. Using methods derived from TOF-SIMS[20], the beam size of the modified 4700 can be calculated by measuring the distance between the 12% and 88% intensity points in a scan across a feature with a chemically distinct edge. From Figure 5C, the intensity of the rubrene at each point was determined, plotted, and fitted with a trend line. I used a cubic function to represent data and, by calculating the distance where the 88% and 12% intensities would fall on the line, I calculated that the spatial resolution was 2.5 µm for these instrument

settings (Figure 9). Afterwards, using optical microscopy, the ablation craters were measured at 2.51 ± 0.35 µm.

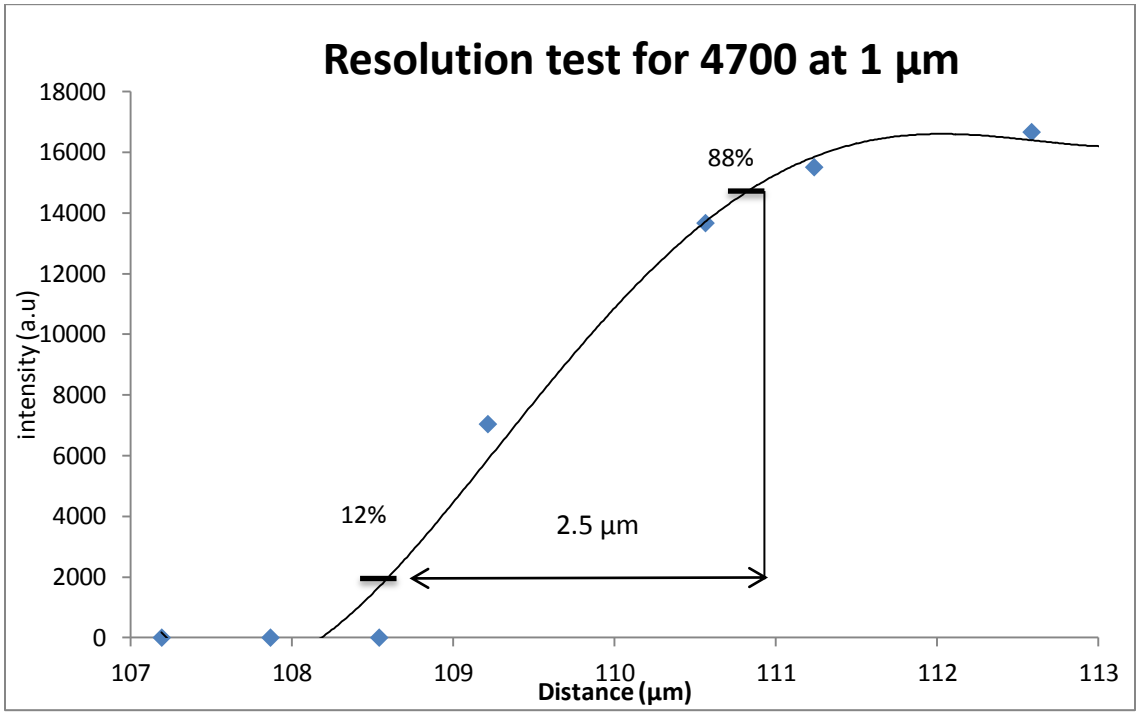

Figure 9: Edge profile of a rubrene feature allowing the measurement of the effective laser size of the modified 4700

Summary

I have shown that the capabilities of this rubrene target include, but are not limited to: simple and reproducible generation, ease of use for the creation of performance evaluations, and multiple measurements taken from a single slide. The ability to generate performance evaluations quickly and easily will allow for standardization across the field. This target enables the comparative measurements and performance evaluations of the accuracy of the positioning

software, accuracy and repeatability of the stepper motors, and accuracy of the laser targeting software to be performed quickly and reliably. I have also shown that the target can be used for multiple instrument platforms, serving as a standard for intra lab comparisons, and also for different instrument manufacturers, serving as a standard across the field.

Biblography

1. Caprioli, R. M.; Farmer, T. B.; Gile, J., Molecular imaging of biological samples: Localization of peptides and proteins using MALDI-TOF MS. *Analytical Chemistry* **1997,** *69* (23), 4751-4760.

2. Grove, K. J.; Frappier, S. L.; Caprioli, R. M., Matrix Pre-Coated MALDI MS Targets for Small Molecule Imaging in Tissues. *Journal of the American Society for Mass Spectrometry* **2011,** *22* (1), 192-195.

3. Seeley, E. H.; Caprioli, R. M., Molecular imaging of proteins in tissues by mass spectrometry. *Proceedings of the National Academy of Sciences of the United States of America* **2008,** *105* (47), 18126-18131.

4. Puolitaival, S. M.; Burnum, K. E.; Cornett, D. S.; Caprioli, R. M., Solvent-free matrix dry-coating for MALDI Imaging of phospholipids. *Journal of the American Society for Mass Spectrometry* **2008,** *19* (6), 882-886.

5. Burnum, K. E.; Cornett, D. S.; Puolitaival, S. M.; Milne, S. B.; Myers, D. S.; Tranguch, S.; Brown, H. A.; Dey, S. K.; Caprioli, R. M., Spatial and temporal alterations of phospholipids determined by mass spectrometry during mouse embryo implantation. *Journal of Lipid Research* **2009,** *50* (11), 2290-2298.

6. Cornett, D. S.; Frappier, S. L.; Caprioli, R. M., MALDI-FTICR imaging mass spectrometry of drugs and metabolites in tissue. *Analytical Chemistry* **2008,** *80* (14), 5648-5653.

7. Manier, M. L.; Reyzer, M. L.; Goh, A.; Dartois, V.; Via, L. E.; Barry, C. E.; Caprioli, R. M., Reagent Precoated Targets for Rapid In-Tissue Derivatization of the Anti-Tuberculosis Drug Isoniazid Followed by MALDI Imaging Mass Spectrometry. *Journal of the American Society for Mass Spectrometry* **2011,** *22* (8), 1409-1419.

8. McLean, J. A.; Ridenour, W. B.; Caprioli, R. M., Profiling and imaging of tissues by imaging ion mobility-mass spectrometry. *Journal of Mass Spectrometry* **2007,** *42* (8), 1099-1105.

9. Senoner, M.; Wirth, T.; Unger, W.; Osterle, W.; Kaiander, I.; Sellin, R. L.; Bimberg, D., BAM-L002 - a new type of certified reference material for length calibration and testing of lateral resolution in the nanometre range. *Surface and Interface Analysis* **2004,** *36* (10), 1423-U9.

10. Choi, J. H.; Kim, D.; Yoo, P. J.; Lee, H. H., Simple detachment patterning of organic layers and its application to organic light-emitting diodes. *Advanced Materials* **2005,** *17* (2), 166-+.

11. Lee, H. M.; Kim, J. J.; Choi, J. H.; Cho, S. O., In Situ Patterning of High-Quality Crystalline Rubrene Thin Films for High-Resolution Patterned Organic Field-Effect Transistors. *Acs Nano* **2011,** *5* (10), 8352-8356.

12. Ohmori, Y., Development of organic light-emitting diodes for electro-optical integrated devices. *Laser & Photonics Reviews* **2010,** *4* (2), 300-310.

13. Hasegawa, T.; Takeya, J., Organic field-effect transistors using single crystals. *Science and Technology of Advanced Materials* **2009,** *10* (2).

14. Qin, D.; Xia, Y.; Whitesides, G. M., Soft lithography for micro- and nanoscale patterning. *Nature Protocols* **2010,** *5* (3), 491-502.

15. Hanson, E. L.; Schwartz, J.; Nickel, B.; Koch, N.; Danisman, M. F., Bonding self-assembled, compact organophosphonate monolayers to the native oxide surface of silicon. *J Am Chem Soc* **2003,** *125* (51), 16074-80.

16. Hankin, J. A.; Barkley, R. M.; Murphy, R. C., Sublimation as a method of matrix application for mass spectrometric imaging. *Journal of the American Society for Mass Spectrometry* **2007,** *18* (9), 1646-1652.

17. Zavalin, A.; Todd, E.; Rawhouser, P.; Yang, J.; Caprioli, R., In preparation.

18. Peterson, D. S., Matrix-free methods for laser desorption/ionization mass spectrometry. *Mass Spectrometry Reviews* **2007,** *26* (1), 19-34.

19. Thomas, A.; Charbonneau, J. L.; Fournaise, E.; Chaurand, P., Sublimation of New Matrix Candidates for High Spatial Resolution Imaging Mass Spectrometry of Lipids: Enhanced Information in Both Positive and Negative Polarities after 1,5-Diaminonapthalene Deposition. *Analytical Chemistry* **2012,** *84* (4); Hagan, N. A.; Smith, C. A.; Antoine, M. D.; Lin, J. S.; Feldman, A. B.; Demirev, P. A., Enhanced In-Source Fragmentation in MALDI-TOF-MS of Oligonucleotides Using 1,5-Diaminonapthalene. *Journal of the American Society for Mass Spectrometry* **2012,** *23* (4).

20. M. Senoner, T. W., W.E.S. Unger, M. Escher, N. Weber, B. Funnemann, B. Kromker, Testing of Lateral Resolution in the Nanometre Range Using the BAM-L002 - Certified Reference Material Application to Tof-SIMS IV and NanoESCA Instruments. *Journal of Surface analysis* **2005,** *12* (2), 78-82.